Manifold Stabilization and Path-Following Control for Flat Systems with Application to a Laboratory Tower Crane

Manifold Stabilization and Path–Following Control for Flat Systems with Application to a Laboratory Tower Crane

Martin Böck[1] and Andreas Kugi[1]

***Abstract*— This paper deals with the stabilization of manifolds for flat systems. Path–following control results as the special case of stabilizing a manifold with dimension one. The target manifold is defined in terms of the components of the flat output. A control strategy is developed which achieves the following objectives. Firstly, the error dynamics, which describe the deviation of the output from the target manifold, are to be asymptotically stabilized. Therefore, if the system is initialized such that all states of the error dynamics are zero, the invariance property holds. This means that in the nominal, undisturbed case the output of the system does not leave the target manifold for all future times. A further objective is that the movement of the system on the target manifold can be appropriately controlled. The degrees of freedom of this movement are given by the dimension of the manifold. Some nice features are gained by the restriction to flat systems. Amongst others, the controller which achieves the objectives of stabilization, invariance, and movement on the manifold can always be calculated in a systematic way. To this end, the equivalence of flat systems to linear controllable ones is exploited. The presented control methodology is applied to a laboratory experiment of a tower crane. The experimental results underline the feasibility of the proposed concept.**

I. INTRODUCTION

Besides the fields of set point stabilization and trajectory tracking control, modern control theory is increasingly dealing with the challenges of manifold stabilization and path–following control.

Stabilizing manifolds can be seen as an extension of the well–known task of set point stabilization (as a set point constitutes a manifold of dimension zero). The manifolds are typically defined in the output or state space of a dynamical system [1]. Roughly speaking, the goal of manifold stabilization is to make the output or state of the system (asymptotically) approach the manifold. Two important properties are frequently considered. Firstly, it is desirable that the movement on the target manifold (tangential movement) can be influenced. Secondly, if the system is initialized exactly on the manifold (or more precisely in a corresponding controlled invariant subset of the state space) then it should stay on the manifold for all future times (in the nominal, undisturbed case) independent of the tangential movement [2]. This property is subsequently referred to as the invariance property.

In [1], [3] the authors investigate the stabilization of controlled invariant submanifolds of the state space of control–affine dynamical systems. Conditions are given for the existence of output functions allowing to perform input–output feedback linearization yielding a so–called transverse normal form (TNF). Roughly speaking, these output functions represent the off–the–manifold movement of the system. For the TNF it is required that the zero dynamics manifold has the same dimension as the manifold to be stabilized and the input–output dynamics (the transverse dynamics) are in Brunovský normal form. As a result, the movement on the target manifold is described by the zero dynamics (the tangential dynamics) and the manifold is stabilized by rendering the origin of the transverse dynamics stable. This can be accomplished in the coordinates of the TNF in a straightforward way.

Path–following control is often seen as a generalization of trajectory tracking control [4]. This can be reasoned based on the fact that both frameworks deal with predefined geometric reference curves (subsequently also referred to as path) but only for trajectory tracking control the time–parameterization of the curve is fixed beforehand. On the contrary, for path–following control it is not defined a priori when the system is expected to pass a specific point of the reference curve. Ideally, the invariance property is fulfilled, i.e. when starting on the path (or in a corresponding controlled invariant subset of the state space) the system stays exactly on the path for all future times [1]. Note that trajectory tracking control does not necessarily share this property [2]. The paths are typically defined in the state space [5], [6] or output space [2], [7] of the system.

Starting from the early works of, e.g., Banaszuk and Hauser [8], several extensions and improvements of path–following control have been proposed in literature. From a geometric point of view, the reference curve poses a one–dimensional manifold which has to be stabilized. Therefore, path–following control can be seen as a special case of manifold stabilization [1]. Other researchers suggest the use of model predictive control (MPC) to solve the problem, cf., e.g., [6], [7], [9]. This has the advantage of being able to systematically take into account system constraints.

The aim of this work is to perform manifold stabilization and path–following control for flat systems [10] which is a property of many physical and technical systems encountered in practice, see, e.g., [10], [11]. The restriction to the special case of flat systems exhibits some nice and practically useful features. Utilizing the flatness property, the system can be transformed to a specific TNF by means of a generalized state transformation without the need for dynamic extension. The term generalized refers to the fact that the state transformation also depends on the new input and its time derivatives. As a result, not only the transverse

[1]M. Böck and A. Kugi are with the Automation and Control Institute, Vienna University of Technology, 1040 Vienna, Austria {boeck,kugi}@acin.tuwien.ac.at

Post-print version of the article: M. Böck and A. Kugi, "Manifold stabilization and path-following control for flat systems with application to a laboratory tower crane", in *Proc. 53rd IEEE Conference on Decision and Control*, Los Angeles, CA, USA, Dec. 2014, pp. 4529–4535. DOI: 10.1109/CDC.2014.7040096

part of the TNF is linear but the whole dynamics, which greatly simplifies the tangential control design. Moreover, we confine ourselves to the stabilization of manifolds in the flat output space, which renders the problem much simpler compared to the general case. In [1], [2], the stabilization of a one–dimensional manifold (curve) in the output space is considered where the motion along the curve shall meet certain application–specific requirements. In order to meet these requirements, the diffeomorphism mapping to TNF has to be completed by suitable functions determining the tangential dynamics. The latter step is circumvented in this work for the stabilization in the flat output space by choosing functions solely depending on the flat output which specify the motion on the target manifold. In [12], a similar approach is employed for one–dimensional paths but with dynamic extension.

The proposed method is applied to a laboratory experiment of a tower crane. The flat output under consideration is given by the Cartesian coordinates of the load. We investigate two test cases. Firstly, path–following control for a geometric path of elliptic shape is conducted. This result could be used for transferring the load from one point in the work space of the crane to another. The movement along the ellipse can be chosen freely. Secondly, a two–dimensional manifold in the form of a vertical plane is considered, i.e. the load is expected to move only in this vertical plane. Again, the movement in the vertical plane can be chosen freely while maintaining the invariance property. The feasibility of the proposed method is demonstrated by means of experimental results from the laboratory tower crane. A video of the presented test cases is available[1].

The paper is organized as follows. In Section II, the problem of manifold stabilization is formulated. The solution of this problem for the considered class of flat systems is presented in Section III. Section IV contains the application of the proposed control concept to the tower crane system.

The notation is as follows. The total derivatives of a quantity y with respect to time t are denoted by $\dot{y}$, $\ddot{y}$, $y^{(3)}$, and so forth. A sequence of derivatives of unknown finite maximum order is denoted by $y, \dot{y}, \ddot{y}, \ldots$. The tuple ${}^{i}x, {}^{i}y, {}^{i}z$ constitutes the coordinates in a coordinate system i with corresponding basis vectors $({}_{i}x, {}_{i}y, {}_{i}z)$. The Lie derivative is written as $(L_f h)(x) = \left(\frac{\partial h}{\partial x}\right) f$ with h possibly vector–valued, i.e. $h(x) \in \mathbb{R}^p$ with $p \geq 1$. The index i refers to the ith component of a vector–valued quantity.

II. PROBLEM STATEMENT

We consider flat systems in the form

$$\dot{x} = f(x, u) \tag{1a}$$
$$y = h(x) \tag{1b}$$

with $x \in \mathbb{R}^n$, $u \in \mathbb{R}^m$, $\operatorname{rank}\left(\frac{\partial f}{\partial u}\right) = m$, and $y \in \mathbb{R}^m$ constituting a flat output. For brevity and clearness of exposition, we consider system equations and output functions (1) which do not depend on derivatives of u. However, all subsequent results can be extended to $\dot{x} = f(x, u, \dot{u}, \ddot{u}, \ldots)$ and $y = h(x, u, \dot{u}, \ddot{u}, \ldots)$. The flat parameterizations of the state and input read as

$$x = \psi_x(y, \dot{y}, \ddot{y}, \ldots) \tag{2a}$$
$$u = \psi_u(y, \dot{y}, \ddot{y}, \ldots). \tag{2b}$$

The manifold to be stabilized (subsequently referred to as the target manifold) is defined in terms of the flat output

$$\mathcal{M} = \{y \in \mathbb{R}^m | \hat{\sigma}(y) = 0\} \tag{3}$$

with a continuous function $\hat{\sigma} : \mathbb{R}^m \to \mathbb{R}^{m-p}$, $0 \leq p \leq m-1$, i.e. the manifold $\mathcal{M}$ has dimension p. The natural requirement for $\hat{\sigma}$ is that

$$\operatorname{rank}\left(\frac{\partial \hat{\sigma}}{\partial y}\right)(\tilde{y}) = m - p \quad \forall \tilde{y} \in \mathcal{M}. \tag{4}$$

Note that for $p = 1$, one obtains as a special case a one–dimensional geometric curve [1], [2], either open or closed, see also [12], [13]. Subsequently, we refer to such a geometric curve as path [1]. Alternatively, the path could also be defined in explicit form as a regular parameterized curve

$$\mathcal{P} = \{\bar{p} \in \mathbb{R}^m | \bar{p} = P(\theta), \ \theta \in \mathbb{R}\} \tag{5}$$

with the path parameter θ and the map $P(\theta)$ either defining a closed or open curve $\mathcal{P}$ [12]. In this case, we assume that the curve (5) admits an implicit representation in the form (3). Thus, we do not distinguish between stabilization of a manifold or a one–dimensional curve (path–following control). The latter is included in the former as a special case. Therefore, we subsequently focus on manifold stabilization for which the control objectives are defined as follows.

O1) Asymptotic convergence to $\mathcal{M}$: The output y of system (1) in the closed–loop satisfies $\|y\|_{\mathcal{M}} \to 0$ for $t \to \infty$, where $\|y\|_{\mathcal{M}}$ denotes the shortest distance of y to the manifold $\mathcal{M}$, i.e. $\|y\|_{\mathcal{M}} = \min_{\bar{y} \in \mathcal{M}} \|\bar{y} - y\|$, cf., e.g., [2].

O2) Invariance property: If the system state $x(t_0)$ at initial time t_0 is contained in an appropriate subset of

$$\Gamma = \{\bar{x} \in \mathbb{R}^n | \hat{\sigma}(h(\bar{x})) = 0\} \tag{6}$$

then the invariance property shall hold, i.e. $\|y(t)\|_{\mathcal{M}} = 0$, $\forall t \geq t_0$.

O3) Tangential movement: Achieve an application–specific motion of y on $\mathcal{M}$ according to its dimension p.

III. MANIFOLD STABILIZATION FOR FLAT SYSTEMS

The goal of this section is to show that for flat systems the control objectives O1–O3 of manifold stabilization can always be achieved in a systematic way. To this end, results from literature concerning the exact linearization of flat systems are shortly repeated in Section III-A. These results are combined with existing ideas and approaches mainly from [1] in Section III-B to solve the problem at hand.

[1] http://www.acin.tuwien.ac.at/fileadmin/cds/videos/craneManStab.wmv

Post-print version of the article: M. Böck and A. Kugi, "Manifold stabilization and path-following control for flat systems with application to a laboratory tower crane", in *Proc. 53rd IEEE Conference on Decision and Control*, Los Angeles, CA, USA, Dec. 2014, pp. 4529–4535.
DOI: 10.1109/CDC.2014.7040096
The content of this post-print version is identical to the published paper but without the publisher's final layout or copy editing.

A. Exact Linearization of Flat Systems

It is a well–known fact that a flat system (1) is equivalent to a linear controllable one in Brunovský normal form [10]

$$y_i^{(\rho_i)} = v_i,\ i = 1, \dots, m \tag{7}$$

with new inputs $v \in \mathbb{R}^m$, the Brunovský state

$$\zeta^{\mathrm{T}} = \begin{bmatrix} y_1 & \dots & y_1^{(\rho_1-1)} & \dots & y_m & \dots & y_m^{(\rho_m-1)} \end{bmatrix}, \tag{8}$$

and positive integers ρ_i. This equivalence can be realized by various types of feedback. One possibility is to utilize a so–called quasi–static state feedback [14] in the form

$$u = \kappa\left(\zeta, v, \dot{v}, \ddot{v}, \dots\right) \tag{9}$$

which follows from (2b) by using (7) and (8). The generalized state transformation linking the system state x with the Brunovský state ζ can be deduced in an analogous fashion and reads as

$$x = \Lambda\left(\zeta, v, \dot{v}, \ddot{v}, \dots\right). \tag{10}$$

The characteristics of the quasi–static approach is that the dimension of the state space of the closed–loop system is equal to the one of the original system, i.e. it holds that $\sum_{i=1}^{m} \rho_i = n$. Due to the fact that in general derivatives of the new input v appear in (9) the feedback is not static but quasi–static. The Brunovský state ζ needed in (9) can be calculated, e.g., from the inversion of (10), see, e.g., [15]. Alternatively to a quasi–static feedback one might use an endogenous dynamic feedback [10] for which the dimension of the state space of the closed–loop system is $\sum_{i=1}^{m} \rho_i > n$.

In the following, we utilize the quasi–static state feedback (9) as it does not require a dynamics in the controller. Nevertheless, the presented results are transferable to the case of endogenous dynamic feedback.

B. Controller Design Methodology for Stabilizing Manifolds in Flat Output Spaces

From a geometric point of view, any movement of the output of the system can be composed of a tangential and a transverse part with respect to the target manifold $\mathcal{M}$ [1]. The transverse part describes the motion off the manifold. If this part is identically zero the output y of the system exactly lies on $\mathcal{M}$. To ensure that the invariance property holds in this case, the motion of the output is locally restricted to the tangent space of the target manifold. In other words, the motion of the output is restricted to a p–dimensional subspace described by the tangential part. Our goal is to obtain a special kind of TNF [1] for system (1) and the given target manifold (3) in order to achieve the objectives O1–O3 formulated in Section II. In the coordinates of the TNF, the transverse and tangential movement of y can be independently controlled by transverse and tangential control inputs [1], [2] and controllers can be designed in a straightforward way.

To this end, we define the function

$$\bar{\sigma}\left(y\right) : \mathbb{R}^m \to \mathbb{R}^p \tag{11}$$

which can be combined with $\hat{\sigma}\left(y\right)$ (defining the target manifold and whose components are (locally) independent) to $\sigma\left(y\right) = \begin{bmatrix} \hat{\sigma}^{\mathrm{T}} & \bar{\sigma}^{\mathrm{T}} \end{bmatrix}^{\mathrm{T}}\left(y\right)$ which is presumed to fulfill

$$\operatorname{rank}\left(\frac{\partial \sigma}{\partial y}\right)\left(\tilde{y}\right) = m \quad \forall \tilde{y} \in \mathcal{M}. \tag{12}$$

The components of $\bar{\sigma}$ can be chosen freely as long as (12) holds, however, the choice strongly depends on the considered application. The function $\bar{\sigma}$ characterizes the movement of the output y of the system on the target manifold $\mathcal{M}$. This is due to (4) and (12). Furthermore, as long as $\hat{\sigma}\left(y\right) = 0$ is fulfilled, the function $\bar{\sigma}\left(y\right)$ can take arbitrary values and the output of the system is in any case on the target manifold. From a practical point of view it is highly convenient to define the function $\bar{\sigma}$ in terms of the system output y.

In order to proceed with the controller design, we consider the new output functions

$$\hat{y} = \hat{\sigma}\left(h\left(x\right)\right) =: \hat{h}\left(x\right) \tag{13a}$$

$$\bar{y} = \bar{\sigma}\left(h\left(x\right)\right) =: \bar{h}\left(x\right) \tag{13b}$$

which allow to define the new system output

$$z = \sigma\left(h\left(x\right)\right) = \begin{bmatrix} \hat{h}\left(x\right) \\ \bar{h}\left(x\right) \end{bmatrix} =: \Upsilon\left(x\right) \in \mathbb{R}^m. \tag{14}$$

Now (14) is also a flat output of (1a) if additionally to (12) all partial derivatives of σ and σ^{-1} up to a certain order are continuous [16]. This enables to perform exact linearization of system (1a) with the new output (14) as explained in Section III-A. The corresponding Brunovský normal form reads as

$$\hat{y}_i^{(\hat{\rho}_i)} = v_i^{\pitchfork},\ i = 1, \dots, m-p \tag{15a}$$

$$\bar{y}_j^{(\bar{\rho}_j)} = v_j^{\parallel},\ j = 1, \dots, p \tag{15b}$$

which constitutes the TNF and it holds that $\sum_{i=1}^{m-p} \hat{\rho}_i + \sum_{j=1}^{p} \bar{\rho}_j = n$ with positive integers $\hat{\rho}_i, \bar{\rho}_j$. The Brunovský state belonging to (15) is given by

$$\zeta^{\mathrm{T}} = \begin{bmatrix} \xi^{\mathrm{T}} & \eta^{\mathrm{T}} \end{bmatrix} \tag{16}$$

with

$$\xi^{\mathrm{T}} = \begin{bmatrix} \hat{y}_1 & \dots & \hat{y}_1^{(\hat{\rho}_1-1)} & \dots & \hat{y}_{m-p} & \dots & \hat{y}_{m-p}^{(\hat{\rho}_{m-p}-1)} \end{bmatrix} \tag{17a}$$

$$\eta^{\mathrm{T}} = \begin{bmatrix} \bar{y}_1 & \dots & \bar{y}_1^{(\bar{\rho}_1-1)} & \dots & \bar{y}_p & \dots & \bar{y}_p^{(\bar{\rho}_p-1)} \end{bmatrix}. \tag{17b}$$

The states ξ correspond to the transverse dynamics (15a) and η contains the states of the tangential dynamics (15b). The number of integrator chains in the tangential dynamics is equal to the dimension p of the target manifold $\mathcal{M}$. Similar to (9) and (10), the quasi–static state feedback follows as

$$u = \kappa\left(\zeta, v^{\pitchfork}, \dot{v}^{\pitchfork}, \ddot{v}^{\pitchfork}, \dots, v^{\parallel}, \dot{v}^{\parallel}, \ddot{v}^{\parallel}, \dots\right) \tag{18}$$

and the generalized state transformation linking x with ζ in general form reads as

$$x = \Lambda\left(\zeta, v^{\pitchfork}, \dot{v}^{\pitchfork}, \ddot{v}^{\pitchfork}, \dots, v^{\parallel}, \dot{v}^{\parallel}, \ddot{v}^{\parallel}, \dots\right) \tag{19}$$

Post-print version of the article: M. Böck and A. Kugi, "Manifold stabilization and path-following control for flat systems with application to a laboratory tower crane", in *Proc. 53rd IEEE Conference on Decision and Control*, Los Angeles, CA, USA, Dec. 2014, pp. 4529–4535. DOI: 10.1109/CDC.2014.7040096
The content of this post-print version is identical to the published paper but without the publisher's final layout or copy editing.

with $v^{\pitchfork} = \begin{bmatrix} v_1^{\pitchfork} & \dots & v_{m-p}^{\pitchfork} \end{bmatrix}^{\mathrm{T}}$ and $v^{\parallel} = \begin{bmatrix} v_1^{\parallel} & \dots & v_p^{\parallel} \end{bmatrix}^{\mathrm{T}}$. In many cases, the inverse mappings

$$\xi = \bar{\Lambda}_1 \left(x, v^{\pitchfork}, \dot{v}^{\pitchfork}, \ddot{v}^{\pitchfork}, \dots, v^{\parallel}, \dot{v}^{\parallel}, \ddot{v}^{\parallel}, \dots \right) \tag{20a}$$

$$\eta = \bar{\Lambda}_2 \left(x, v^{\pitchfork}, \dot{v}^{\pitchfork}, \ddot{v}^{\pitchfork}, \dots, v^{\parallel}, \dot{v}^{\parallel}, \ddot{v}^{\parallel}, \dots \right) \tag{20b}$$

are explicitly available too, cf. Section IV.

Remark 1: Note that if the output (14) has some vector relative degree [17] $\{r_1, \dots, r_m\}$ with $\sum_{i=1}^m r_i = n$ then the results analogously hold as (1a) with output (14) is full state linearizable by means of static state feedback [18]. This implicates that (14) is a flat output and therefore this case is included in the presented framework. However, in this case (19) does not depend on $v^{\pitchfork}$, $v^{\parallel}$ and derivatives of $v^{\pitchfork}$ and $v^{\parallel}$ do neither appear in (18) nor in (19).

Concerning the control objectives from Section II, it is obvious that O1 can be achieved by designing a controller rendering the transverse dynamics (15a) asymptotically stable. Objective O3 can be accomplished by a suitable choice of $\bar{\sigma}(y)$ and designing an appropriate controller for (15b). The controller design for both objectives can be carried out in a straightforward way as (15) is linear and controllable. Objective O2 addresses the invariance property. Apparently, if $x(t_0)$ is contained in Γ according to (6) then $y(t_0) \in \mathcal{M}$ is fulfilled. However, note that in general Γ is not controlled invariant [1], [17] thus inducing that $\mathcal{M}$ might be left and approached again. In view of (15a) the following condition can be deduced. If $x(t_0)$ is such that $\xi(t_0) = 0$ then the invariance property (objective O2) is obviously fulfilled by choosing $v^{\pitchfork} \equiv 0$. This is not contrary to objectives O1 and O3 as a controller rendering (15a) asymptotically stable has to fulfill $v^{\pitchfork} \equiv 0$ for $\xi(t_0) = 0$ and regulating (15b) by a proper choice of $v^{\parallel}$ does not influence (15a). However, the choice of controllers for achieving O1 and O3 in general affects the set of initial conditions for which $\xi(t_0) = 0$ holds as $v^{\pitchfork}$ and $v^{\parallel}$ together with its derivatives appear in (20a). Therefore, for a specific application, the control laws have to be inserted into (20a) to check if $\xi(t_0) = 0$ holds for the given initial condition $x(t_0)$ (and thus if the invariance property is fulfilled).

IV. APPLICATION TO A LABORATORY TOWER CRANE

In this section, a laboratory experiment of a tower crane serves as test case for the presented framework of manifold stabilization and path–following control. The description of the system and the corresponding mathematical model are shortly presented. For details regarding the derivation of the mathematical model and the overall control structure, see [9].

A. Tower Crane System

The considered laboratory tower crane is shown in Fig. 1. It is an underactuated mechanical system with five degrees of freedom (DOF) which are given by the position s_1 of the trolley along the jib, the length s_2 of the cable from the trolley to the load, the angular displacement ϕ_1 of the jib,

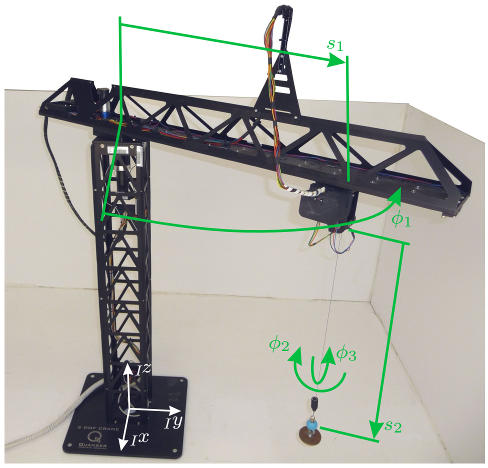

Fig. 1. Tower crane system.

and the angular displacements ϕ_2 and ϕ_3 of the cable with respect to the trolley. Three DOF are actuated (s_1, s_2, and ϕ_1) by means of DC motors while ϕ_2 and ϕ_3 are unactuated. The DC motors are equipped with fast underlying current controllers. In order to have the whole state of the system available for feedback control, all five DOF are directly measured by means of incremental encoders. Approximate differentiation and an observer are employed to obtain the corresponding velocities $\dot{s}_1$, $\dot{s}_2$, $\dot{\phi}_1$, $\dot{\phi}_2$, and $\dot{\phi}_3$. To allow the cable to sway in any direction, it is guided on the trolley by means of a sleeve mounted on a gimbal which has a vertical distance of $h = 0.92\,\mathrm{m}$ to the ground of the workspace. The angular displacements ϕ_2 and ϕ_3 of the cable are measured by the angular displacements of the sleeve. However, to reduce friction, the guidance of the cable in the sleeve is not completely tight. This loose guidance inherently introduces measurement errors, which will become apparent in Section IV-E.

B. Mathematical Model and Flat Output

The laboratory experiment suffers from considerable friction effects. To compensate for the friction in the actuated DOF and to be independent of the actual value of the load mass, it is advantageous to use velocity controllers for each of the actuated DOF. Under the reasonable assumption [9] that the dynamics of the subordinate velocity control loops are negligible, application of Lagrange's formalism yields the mathematical model of the crane in control–affine form

$$\dot{x} = f(x) + g(x)\,u \tag{21}$$

with the control input $u \in \mathbb{R}^3$ given by the accelerations $\ddot{s}_1$, $\ddot{s}_2$, $\ddot{\phi}_1$ of the three actuated DOF and the state $x = \begin{bmatrix} s_1 & s_2 & \phi_1 & \phi_2 & \phi_3 & \dot{s}_1 & \dot{s}_2 & \dot{\phi}_1 & \dot{\phi}_2 & \dot{\phi}_3 \end{bmatrix}^{\mathrm{T}}$. The explicit equations behind (21) are omitted for brevity but can be found in [9]. The actual desired velocities for the subordinate velocity controllers are generated by discrete–time integrators. The flat output y of interest is given by the

Post-print version of the article: M. Böck and A. Kugi, "Manifold stabilization and path-following control for flat systems with application to a laboratory tower crane", in *Proc. 53rd IEEE Conference on Decision and Control*, Los Angeles, CA, USA, Dec. 2014, pp. 4529–4535. DOI: 10.1109/CDC.2014.7040096

load position in the inertial coordinate system $({}_Ix, {}_Iy, {}_Iz)$

$$y = \begin{bmatrix} y_1 \\ y_2 \\ y_3 \end{bmatrix} = \begin{bmatrix} {}^Ix \\ {}^Iy \\ {}^Iz \end{bmatrix} = h\left(x\right) = \begin{bmatrix} s_1\cos(\phi_1) \\ s_1\sin(\phi_1) \\ 0 \end{bmatrix} \tag{22}$$
$$+ \begin{bmatrix} -s_2\left(\sin(\phi_1)\sin(\phi_3) + \cos(\phi_1)\sin(\phi_2)\cos(\phi_3)\right) \\ s_2\left(\cos(\phi_1)\sin(\phi_3) - \sin(\phi_1)\sin(\phi_2)\cos(\phi_3)\right) \\ h - s_2\cos(\phi_2)\cos(\phi_3) \end{bmatrix}.$$

C. Path–Following Control for a Path of Elliptic Shape

The considered task of path–following control at the tower crane is to make the load position approach and follow a curve of elliptic shape. The ellipse is defined with an arbitrary position and rotation in the inertial coordinate system $({}_Ix, {}_Iy, {}_Iz)$. To this end, consider the coordinate system $({}_3x, {}_3y, {}_3z)$ whose ${}_3y$– and ${}_3z$–axes are parallel to the major axes I and II of the ellipse, resp. Thus, the implicit definition of the ellipse reads as

$$\frac{\left({}^3y - l_0\right)^2}{a^2} + \frac{\left({}^3z - l_1\right)^2}{b^2} - 1 = 0 \quad \text{and} \quad {}^3x - l_2 = 0 \tag{23}$$

with $a, b > 0$ denoting the lengths of the major axes. The ellipse lies in a plane parallel to the ${}_3y$–${}_3z$–plane with a distance $l_2 \neq 0$ away. The displacement of the center of the ellipse in ${}_3y$– and ${}_3z$–direction is given by $l_0, l_1 \in \mathbb{R}$.

The $({}_3x, {}_3y, {}_3z)$ coordinate system can have an arbitrary rotation with respect to the inertial frame $({}_Ix, {}_Iy, {}_Iz)$ described by the Tait–Bryan angles α, β, γ and the corresponding rotation matrix A_{I3} with the coordinate transformation

$$y = A_{I3}\begin{bmatrix}{}^3x & {}^3y & {}^3z\end{bmatrix}^{\mathrm{T}} \Rightarrow \begin{bmatrix}{}^3x & {}^3y & {}^3z\end{bmatrix}^{\mathrm{T}} = A_{I3}^{\mathrm{T}}y. \tag{24}$$

Inserting the relation (24) into (23) yields the function $\hat{\sigma} : \mathbb{R}^3 \to \mathbb{R}^2$ defining the path according to (3)

$$\hat{\sigma}\left(y\right) = \begin{bmatrix} \hat{\sigma}_1\left(y\right) \\ y_1\cos\alpha\cos\beta + y_2\sin\alpha\cos\beta - y_3\sin\beta - l_2 \end{bmatrix}. \tag{25}$$

For the sake of brevity $\hat{\sigma}_1(y)$ is not stated explicitly. As outlined in Section III-B, one more scalar function $\bar{\sigma}(y)$ describing the motion on the path can be chosen. For the considered case, it is interesting to be able to directly influence the position of the load along the ellipse. This position can be conveniently described by the angle μ between the ray from the center of the ellipse to any point on the ellipse and the major axis I. This angle is given by $\mu = \arctan\left(\frac{{}^3z - l_1}{{}^3y - l_0}\right)$ and by inserting (24) one obtains

$$\mu|_{\left[{}^3x \;\; {}^3y \;\; {}^3z\right]^{\mathrm{T}} = A_{I3}^{\mathrm{T}}y} = \bar{\sigma}\left(y\right) : \mathbb{R}^3 \to \mathbb{R}. \tag{26}$$

It can be verified that (12) is fulfilled with $m = 3$ and that

$$z = \Upsilon\left(x\right) = \begin{bmatrix} \hat{y} \\ \bar{y} \end{bmatrix} = \begin{bmatrix} \hat{\sigma}\left(h\left(x\right)\right) \\ \bar{\sigma}\left(h\left(x\right)\right) \end{bmatrix} \tag{27}$$

according to (14) is again a flat output as required in Section III-B. Based on (27), we are able to define objective O3 for the considered application. It is required that $\bar{y}(t)$ (asymptotically) tracks a desired reference profile $\bar{y}_d(t)$. Subsequently, one possible way is shown how to calculate the quasi–static state feedback

$$u = \kappa\left(x, v^{\pitchfork}, \dot{v}^{\pitchfork}, \ddot{v}^{\pitchfork}, \ldots, v^{\parallel}, \dot{v}^{\parallel}, \ddot{v}^{\parallel}, \ldots\right) \tag{28}$$

and the corresponding transformations (20) to TNF (15). Note that, contrary to (18), we seek for the quasi–static feedback (28) directly in terms of the original system state x instead of ζ.

To this end, we successively differentiate (27)

$$\dot{z} = \left(L_f\Upsilon\right)\left(x\right) + \underbrace{\left(L_g\Upsilon\right)\left(x\right)}_{0}u \tag{29a}$$
$$\ddot{z} = \left(L_f^2\Upsilon\right)\left(x\right) + \left(L_g\left(L_f\Upsilon\right)\right)\left(x\right)u \tag{29b}$$

where in the second derivative $\ddot{z}$ the input u appears. However, the rank of the decoupling matrix $\left(L_g\left(L_f\Upsilon\right)\right)(x)$ is only 1 for generic values of x. Thus, u_2 is chosen such that $\ddot{z}_1 = v_1^{\pitchfork}$ holds, which results in

$$u_2 = \frac{1}{\left(L_{g_2}\left(L_f\Upsilon_1\right)\right)\left(x\right)}\Big(v_1^{\pitchfork} - \left(L_f^2\Upsilon_1\right)\left(x\right) \tag{30}$$
$$- \textstyle\sum_{i\in\{1,3\}}\left(L_{g_i}\left(L_f\Upsilon_1\right)\right)\left(x\right)u_i\Big) =: \bar{\kappa}\left(x, u_1, u_3, v_1^{\pitchfork}\right).$$

Inserting (30) into the two remaining components of $\ddot{z}$ yields

$$Z = \begin{bmatrix}\ddot{z}_2 \\ \ddot{z}_3\end{bmatrix}\Bigg|_{u_2=\bar{\kappa}} = \chi\left(x, v_1^{\pitchfork}\right) := \begin{bmatrix}\left(L_f^2\Upsilon_2\right)\left(x\right) \\ \left(L_f^2\Upsilon_3\right)\left(x\right)\end{bmatrix} \tag{31}$$
$$+ \underbrace{\begin{bmatrix}\frac{\left(L_{g_2}\left(L_f\Upsilon_2\right)\right)\left(x\right)}{\left(L_{g_2}\left(L_f\Upsilon_1\right)\right)\left(x\right)} & \frac{\left(L_{g_2}\left(L_f\Upsilon_3\right)\right)\left(x\right)}{\left(L_{g_2}\left(L_f\Upsilon_1\right)\right)\left(x\right)}\end{bmatrix}^{\mathrm{T}}}_{\delta(x)}\left(v_1^{\pitchfork} - \left(L_f^2\Upsilon_1\right)\left(x\right)\right)$$

with the property $\left(L_g\delta\right)(x) = 0$ and all terms with u_1, u_3 vanishing due to $\operatorname{rank}\left(L_g\left(L_f\Upsilon\right)\right)(x) = 1$. Again, by differentiating (31) and inserting (30) one obtains

$$\dot{Z} = \left(L_f\chi\right)\left(x, v_1^{\pitchfork}\right) + \frac{\left(L_{g_2}\chi\right)\left(x\right)}{\left(L_{g_2}\left(L_f\Upsilon_1\right)\right)\left(x\right)}\left(v_1^{\pitchfork} - \left(L_f^2\Upsilon_1\right)\left(x\right)\right)$$
$$+ \delta\left(x\right)\dot{v}_1^{\pitchfork} =: \bar{\chi}\left(x, v_1^{\pitchfork}, \dot{v}_1^{\pitchfork}\right), \tag{32}$$

where again all terms with u_1 and u_3 cancel each other out. The next derivative results in

$$\ddot{Z} = \bar{\bar{\chi}}\left(x, v_1^{\pitchfork}, \dot{v}_1^{\pitchfork}, \ddot{v}_1^{\pitchfork}\right) + D\left(x, v_1^{\pitchfork}\right)\begin{bmatrix}u_1 & u_3\end{bmatrix}^{\mathrm{T}} \tag{33}$$

with $\operatorname{rank} D\left(x, v_1^{\pitchfork}\right) = 2$ at generic points. By imposing $\ddot{Z}_1 = z_2^{(4)} = v_2^{\pitchfork}$ and $\ddot{Z}_2 = z_3^{(4)} = v^{\parallel}$ one obtains

$$\begin{bmatrix}u_1 \\ u_3\end{bmatrix} = D^{-1}\left(x, v_1^{\pitchfork}\right)\left\{\begin{bmatrix}v_2^{\pitchfork} \\ v^{\parallel}\end{bmatrix} - \bar{\bar{\chi}}\left(x, v_1^{\pitchfork}, \dot{v}_1^{\pitchfork}, \ddot{v}_1^{\pitchfork}\right)\right\}. \tag{34}$$

The quasi–static state feedback (30) and (34) transforms the system (21), (27) to TNF

$$\hat{y}_1^{(2)} = v_1^{\pitchfork} \qquad \hat{y}_2^{(4)} = v_2^{\pitchfork} \tag{35a}$$
$$\bar{y}^{(4)} = v^{\parallel}. \tag{35b}$$

Post-print version of the article: M. Böck and A. Kugi, "Manifold stabilization and path-following control for flat systems with application to a laboratory tower crane", in *Proc. 53rd IEEE Conference on Decision and Control*, Los Angeles, CA, USA, Dec. 2014, pp. 4529–4535. DOI: 10.1109/CDC.2014.7040096
The content of this post-print version is identical to the published paper but without the publisher's final layout or copy editing.

The generalized state transformation is directly given by (27), (29a), (31), and (32)

$$\xi = \begin{bmatrix} \xi_{11} \\ \xi_{12} \\ \xi_{21} \\ \xi_{22} \\ \xi_{23} \\ \xi_{24} \end{bmatrix} = \begin{bmatrix} \Upsilon_1(x) \\ (L_f \Upsilon_1)(x) \\ \Upsilon_2(x) \\ (L_f \Upsilon_2)(x) \\ \chi_1\left(x, v_1^{\pitchfork}\right) \\ \bar{\chi}_1\left(x, v_1^{\pitchfork}, \dot{v}_1^{\pitchfork}\right) \end{bmatrix}, \quad \eta = \begin{bmatrix} \Upsilon_3(x) \\ (L_f \Upsilon_3)(x) \\ \chi_2\left(x, v_1^{\pitchfork}\right) \\ \bar{\chi}_2\left(x, v_1^{\pitchfork}, \dot{v}_1^{\pitchfork}\right) \end{bmatrix}. \tag{36}$$

Objectives O1 and O2 are achieved by rendering the transverse dynamics (35a) asymptotically stable. This is accomplished by means of the feedback laws

$$v_1^{\pitchfork} = -k_{10} \int_{t_0}^{t} \xi_{11} \mathrm{d}t - k_{11}\xi_{11} - k_{12}\xi_{12} \tag{37a}$$

$$v_2^{\pitchfork} = -k_{20} \int_{t_0}^{t} \xi_{21} \mathrm{d}t - \sum_{i=1}^{4} k_{2i}\xi_{2i} \tag{37b}$$

with the required derivatives

$$\dot{v}_1^{\pitchfork} = -k_{10}\xi_{11} - k_{11}\xi_{12} - k_{12}v_1^{\pitchfork} \tag{38a}$$

$$\ddot{v}_1^{\pitchfork} = -k_{10}\xi_{12} - k_{11}v_1^{\pitchfork} - k_{12}\dot{v}_1^{\pitchfork}. \tag{38b}$$

For objective O3 to hold, the following control law is utilized

$$v^{\parallel} = \bar{y}_d^{(4)}(t) - k_{30} \int_{t_0}^{t} \left(\eta_1 - \bar{y}_d(t)\right) \mathrm{d}t - \sum_{i=1}^{4} k_{3i} \left(\eta_i - \bar{y}_d^{(i-1)}(t)\right). \tag{39}$$

Integral action is added in all feedback laws (37) and (39) in order to better cope with the non–ideal behavior of the laboratory experiment. The required quantities ξ_{ij} and η_i in (37), (38), and (39) follow from (36). By inserting (37), (38), and (39) into (30) and (34) the final state feedback for path–following control achieving objectives O1–O3 is obtained.

D. Stabilization of a Manifold in the Form of a Plane

As a second task, we consider the stabilization of a manifold in the form of a vertical plane in the workspace of the crane. Thus, $p = 2$ and the function $\hat{\sigma} : \mathbb{R}^3 \to \mathbb{R}$ reads as

$$\hat{\sigma}(y) = L_1 y_1 + L_2 y_2 + L_3 \tag{40}$$

with $L_3 \neq 0$ and L_1 and L_2 not simultaneously equal to zero. Defining the function

$$\bar{\sigma}(y) = \begin{bmatrix} \arctan\left(\frac{y_2}{y_1}\right) & y_3 \end{bmatrix}^{\mathrm{T}} \tag{41}$$

allows to intuitively influence the position of the load in the plane by means of the angle to the ${}_I x$–axis and the vertical position ${}^I z$. Again, it can be verified that (12) is fulfilled. Objective O3 is specialized to the (asymptotic) tracking of a set point $\bar{\sigma}_d = \text{const.}$ The calculations for obtaining a feedback in the form (28) are very similar to Section IV-C and are omitted for brevity. One ends up with a TNF

$$\hat{y}^{(4)} = v^{\pitchfork} \qquad \bar{y}_1^{(4)} = v_1^{\parallel} \qquad \bar{y}_2^{(2)} = v_2^{\parallel} \tag{42}$$

and $v^{\pitchfork}$, $v_1^{\parallel}$, and $v_2^{\parallel}$ are chosen analogously to (37) and (39).

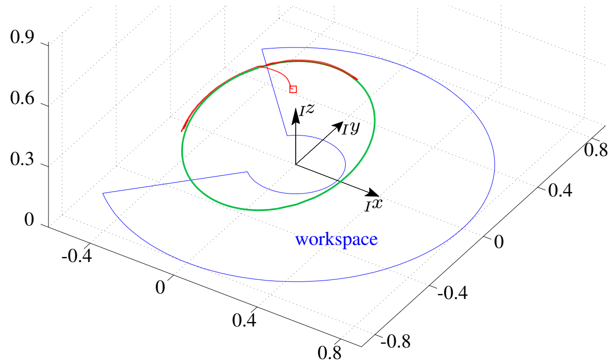

Fig. 2. Workspace of the tower crane with the ellipse to be stabilized and the trajectory of the load (all quantities in m).

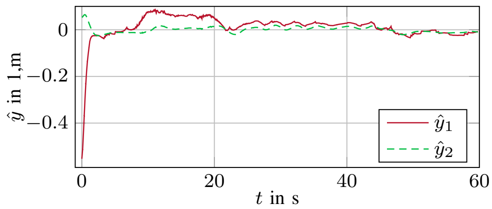

Fig. 3. Virtual system output $\hat{y}$ for PFE.

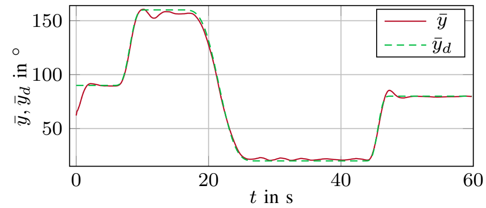

Fig. 4. Virtual system output $\bar{y}$ and $\bar{y}_d(t)$ for PFE.

E. Experimental Results

The controllers derived in Section IV-C and IV-D for path–following along an ellipse (PFE) and stabilization of a vertical plane (SVP) are applied to the laboratory tower crane depicted in Fig. 1. The whole setup is the same as described in [9]. The controllers are executed with a sampling time of 1 ms. The parameters are chosen as $a = 0.4\,\mathrm{m}$, $b = 0.3\,\mathrm{m}$, $\alpha = -45°$, $\beta = -20°$, $\gamma = 10°$, $l_0 = -0.1\,\mathrm{m}$, $l_1 = 0.3\,\mathrm{m}$, $l_2 = 0.5\,\mathrm{m}$, $L_1 = 0.6\,\mathrm{m}$, $L_2 = 1\,\mathrm{m}$, $L_3 = -0.5\,\mathrm{m}$, and the feedback gains k_{ij} are obtained from an LQR design.

Figure 2 shows the ellipse to be stabilized for PFE. Additionally, the corresponding trajectory of the load is depicted which (due to a lack of appropriate sensors) is obtained by inserting the measurements for the state x into (22). The load starts at a position off the target manifold marked with a square. The initial deviation is quickly compensated for by driving the load to the ellipse. This can also be inferred from Fig. 3 showing the virtual system output $\hat{y}$ which is quickly converging to zero. The desired four times continuously differentiable trajectory $\bar{y}_d(t)$ for the angle μ along the ellipse is depicted together with $\bar{y}$ in Fig. 4. Initially, the desired angle along the ellipse has a value of 90° which

Post-print version of the article: M. Böck and A. Kugi, "Manifold stabilization and path-following control for flat systems with application to a laboratory tower crane", in *Proc. 53rd IEEE Conference on Decision and Control*, Los Angeles, CA, USA, Dec. 2014, pp. 4529–4535.
DOI: 10.1109/CDC.2014.7040096

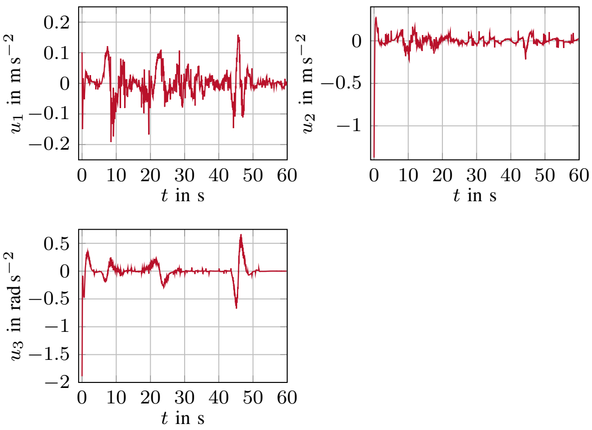

Fig. 5. Control input u for PFE.

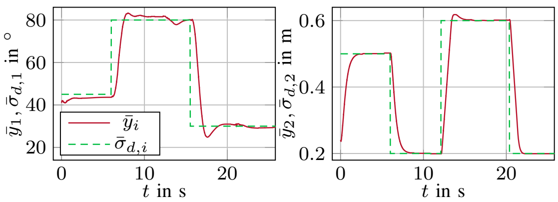

Fig. 6. Virtual system output $\bar{y}$ and $\bar{\sigma}_d$ for SVP.

is quickly reached by $\bar{y}$. At $t \approx 5.6\,\mathrm{s}$ the desired angle is increased to a value of $160°$. Afterwards, it is reduced to $20°$ and finally reaches $80°$. The desired trajectory $\bar{y}_d(t)$ is tracked quite well and the resulting motion in the upper half of the ellipse is visible in Fig. 2. Figure 5 shows the control input u for the described scenario. While traversing the ellipse, $\hat{y}$ shows small deviations from zero (cf. Fig. 3) which result from the loose guidance of the cable in the sleeve attached to the gimbal (cf. Section IV-A) and from sticktion effects.

Concerning SVP, a sequence of set points $\bar{\sigma}_d$ according to Fig. 6 is specified starting with $\bar{\sigma}_d = \begin{bmatrix} 45° & 0.5\,\mathrm{m} \end{bmatrix}^{\mathrm{T}}$. The trajectory of the load can be seen in Fig. 7. Again, the load starts at a position off the target manifold marked with a square. Firstly, the initial deviation is compensated which can be seen in Figs. 6 and 7. Subsequently, the further set points $\bar{\sigma}_d$ are tracked while keeping the load in the vertical plane. The resulting direction of moving is indicated with arrows in Fig. 7. Small deviations from the plane are visible which are mainly due to the inaccurate measurement of ϕ_2 and ϕ_3.

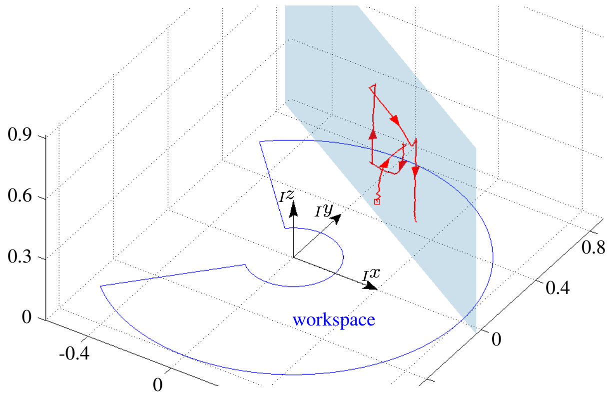

Fig. 7. Workspace of the tower crane with the vertical plane to be stabilized and the trajectory of the load (all quantities in m).

References

[1] C. Nielsen, "Set stabilization using transverse feedback linearization," Ph.D. dissertation, University of Toronto, 2009.

[2] C. Nielsen, C. Fulford, and M. Maggiore, "Path following using transverse feedback linearization: Application to a maglev positioning system," *Automatica*, vol. 46, no. 3, pp. 585–590, 2010.

[3] C. Nielsen and M. Maggiore, "On local transverse feedback linearization," *SIAM Journal on Control and Optimization*, vol. 7, no. 5, pp. 2227–2250, 2008.

[4] A. P. Aguiar, D. B. Dačić, J. P. Hespanha, and P. Kokotović, "Path-following or reference-tracking? An answer relaxing the limits to performance," in *Proc. 5th IFAC/EURON Symposium on Intelligent Autonomous Vehicles (IAV)*, Lisbon, Portugal, July 2004, pp. 179–184.

[5] T. Faulwasser, B. Kern, and R. Findeisen, "Model predictive path-following for constrained nonlinear systems," in *Proc. 48th IEEE Conference on Decision and Control and 28th Chinese Control Conference CDC/CCC*, Shanghai, P.R. China, Dec. 2009, pp. 8642–8647.

[6] S. Yu, X. Li, H. Chen, and F. Allgöwer, "Nonlinear model predictive control for path following problems," in *Proc. 4th IFAC Nonlinear Model Predictive Control Conference*, Noordwijkerhout, Netherlands, Aug. 2012, pp. 145–150.

[7] T. Faulwasser and R. Findeisen, "Constrained output path-following for nonlinear systems using predictive control," in *Proc. 8th IFAC Symposium on Nonlinear Control Systems (NOLCOS)*, Bologna, Italy, Sept. 2010, pp. 753–758.

[8] A. Banaszuk and J. Hauser, "Feedback linearization of transverse dynamics for periodic orbits," *Systems & Control Letters*, vol. 26, no. 2, pp. 95–105, 1995.

[9] M. Böck and A. Kugi, "Real-time nonlinear model predictive path-following control of a laboratory tower crane," *IEEE Trans. Contr. Syst. Technol.*, vol. 22, no. 4, pp. 1461–1473, 2014.

[10] M. Fliess, J. Lévine, P. Martin, and P. Rouchon, "Flatness and defect of non-linear systems: introductory theory and examples," *International Journal of Control*, vol. 61, no. 6, pp. 1327–1361, 1995.

[11] ——, "A Lie–Bäcklund approach to equivalence and flatness of nonlinear systems," *IEEE Trans. Automat. Contr.*, vol. 44, no. 5, pp. 922–937, 1999.

[12] A. Akhtar and C. Nielsen, "Path following for a car-like robot using transverse feedback linearization and tangential dynamic extension," in *Proc. 50th IEEE Conference on Decision and Control and European Control Conference*, Orlando, FL, USA, Dec. 2011, pp. 7974–7979.

[13] A. Akhtar, S. L. Waslander, and C. Nielsen, "Path following for a quadrotor using dynamic extension and transverse feedback linearization," in *Proc. 51st IEEE Conference on Decision and Control*, Maui, Hawaii, USA, Dec. 2012, pp. 3551–3556.

[14] E. Delaleau and J. Rudolph, "Control of flat systems by quasi-static feedback of generalized states," *International Journal of Control*, vol. 71, no. 5, pp. 745–765, 1998.

[15] T. Heyden and C. Woernle, "Dynamics and flatness-based control of a kinematically undetermined cable suspension manipulator," *Multibody System Dynamics*, vol. 16, no. 2, pp. 155–177, 2006.

[16] J. Lévine, *Analysis and Control of Nonlinear Systems - A Flatness-based Approach*, ser. Mathematical Engineering. Berlin, Heidelberg: Springer, 2009.

[17] A. Isidori, *Nonlinear Control Systems*, 3rd ed. London: Springer, 1995.

[18] S. Sastry, *Nonlinear Systems: Analysis, Stability and Control.* New York: Springer, 1999.

Post-print version of the article: M. Böck and A. Kugi, "Manifold stabilization and path-following control for flat systems with application to a laboratory tower crane", in *Proc. 53rd IEEE Conference on Decision and Control*, Los Angeles, CA, USA, Dec. 2014, pp. 4529–4535. DOI: 10.1109/CDC.2014.7040096
The content of this post-print version is identical to the published paper but without the publisher's final layout or copy editing.